UWB radar-based human target tracking

SangHyun Chang[1], Rangoli Sharan[1], Michael Wolf[1], Naoki Mitsumoto[2], Joel W. Burdick[1]
[1]Engineering & Applied Science, California Institute of Technology, MC 104-44, Pasadena, CA 91125, USA
[2]Research laboratories, DENSO Corporation, Aichi, Japan
{sanghyun,rsharan,wolf}@caltech.edu, naoki_mitsumoto@denso.co.jp, jwb@robotics.caltech.edu

***Abstract*— This paper presents a framework and algorithms for tracking the range of moving humans via a mono-static ultra-wideband (UWB) radar. The approach is based on a specular multi-path model for UWB radar scatters from walking humans. Empirical studies show that multipath time-of-arrival (TOA) can be modeled as a point process whose behavior is governed by a Gamma distribution. Based on this insight, we develop a tracking procedure that combines a Kalman Filter with a point process observation model whose measurements are processed with an Expectation-Maximization (EM) procedure. As a byproduct, the EM procedure solves the multi-target data segmentation and data association problems. We present experimental results in which a monostatic UWB radar tracks both individual and up to two human targets.**

***Index Terms*— UWB radar, tracking, filtering**

I. Introduction

This paper introduces a framework and algorithms for tracking the movements of walking humans via mono-static ultra-wideband (UWB) radar. Because the ability to track human movement is useful for wide ranging security and safety applications, a number of technologies have been explored for detecting and tracking humans. While computer vision offers many advantages, it has limited performance in poor visibility conditions (e.g., at night, in haze or fog or smoke). The performance of infrared imaging systems is temperature dependent. Human LADAR signatures are often not highly discriminable from other moving clutter, and LADAR performance degrades in dusty and foggy conditions. UWB radar can provide a complementary technology for detecting and tracking humans, particularly in poor visibility or through-wall conditions. A companion paper [1] develops an algorithm for detecting human presence via UWB radar. This paper presents a novel approach for tracking human targets.

Target tracking using RF, microwave, and mm-wave radar is a well developed subject [2], [3]. The use of UWB radar to track moving objects has been less well investigated [4], [5]. However, UWB radar is perhaps a natural technology for human tracking. Besides its advantages in poor visibility and through wall conditions, the fine temporal resolution afforded by wide bandwidth signals enables high-resolution ranging and localization [6]. Moreover, the scattering pattern of UWB pulses from a human is quite sensitive to the body's dynamically evolving posture [1]. This paper makes the novel observation that the time-of-arrival (TOA) parameters of a multi-path scatter from a walking human can be interpreted as a point process governed by a Gamma distribution. Based on this observation, we develop a tracking framework that combines a Kalman Filter (KF) with a point process observation model that is processed via an Expectation-Maximization (EM) procedure. As a byproduct, the EM procedure naturally solves data segmentation and data association problems.

The authors greatly appreciate the financial support of this work provided by the Denso Corporation, Aichi, Japan.

Section II summarizes a simple multipath signal model that underlies our approach and reviews the CLEAN algorithm for multipath signal deconvolution. Section III shows that scattering path delays can be interpreted as a point process governed by a Gamma distribution. For simplicity of exposition, Section IV shows how to track a single human via a combined KF and Maximum Likelihood (ML) procedure. To handle multiple targets, the ML procedure is extended to an EM procedure in Section V. Sections IV and V also present experimental results to illustrate our approach. Section VI describes ongoing work.

II. Specular Multipath Model for UWB Signal

The UWB radar signal scattered from a human body includes multiple path components, as the impinging UWB electromagnetic wave scatters from different human body parts at different times with various amplitudes (depending on the distance to the body part, and the size and material of the reflecting part). Thus, the returned UWB radar signal $w(t)$ can be approximated by a *specular multipath model* [7]:

$$w(t) \approx \sum_{j=1}^{L} a_j p(t - n_j), \tag{1}$$

with a_j and n_j respectively representing the amplitude and time-of-arrival (TOA) of the j^{th} component of the received signal, and $p(t)$ is an elementary waveform shape, e.g., the transmitted radar waveform in free space. For example, the waveform is recorded over an interval $t \in [t_0, t_{max}]$, which corresponds to a range of $r \in [r_0, r_{max}] = [ct_0/2, ct_{max}/2]$, where c is the speed of light (See details in [1]). The specular multipath model is an approximation whose simplicity allows for real-time processing without compromising UWB radar's high time-resolution capability.

The CLEAN algorithm (CA) [8] can estimate each path's TOA and amplitude, provided a waveform template.

CLEAN Algorithm Summary

1. Input : Waveform shape template $v(t)$; and detection threshold T_{clean} normalized at 1 meter.
2. Initialize : Form initial residual waveform $d_0(t) = w(t)$ for

978-1-4244-2871-7/09/$25.00 ©2009 IEEE

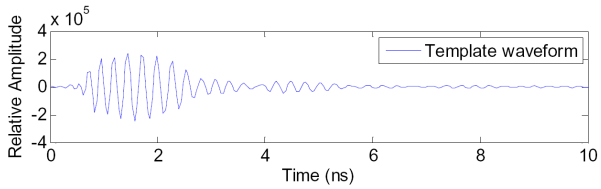

Fig. 1. A template waveform measured at a 1 m T-R separation [1].

a scan. Set counter $i = 0$.

3. Signal Detection : Compute cross-correlation $r_{vd}(\tau)$ between $v(t)$ and $d_i(t)$; the time-index associated to the maximum magnitude of $r_{vd}(\tau)$ is the i^{th} estimated TOA:

$$\hat{n}_i(t) = \arg\max_\tau |r_{vd}(\tau)|.$$

The cross-correlation at $\hat{n}_i(t)$ is the i^{th} estimated amplitude:

$$\hat{a}_i(t) = r_{vd}(\hat{n}_i(t)).$$

If the path magnitude is below the threshold at the TOA, STOP.

4. Increment the iteration counter : $i \leftarrow i + 1$.

5. Residual waveform update:

$$d_i(t) = d_{i-1}(t) - \hat{a}_i(t)v(t - \hat{n}_i(t)).$$

6. Iterate : Go to step 3.

Since UWB radar scatters from both stationary and moving objects, all scatters obtained from a complex test environment must be analyzed for human target candidates. To reduce the high computational cost associated to such analysis, a *moving target indication* (MTI) system, summarized in a companion paper [1], is used to eliminate highly human-unlike scatters.

III. Characterization of Scattered Waveforms from Moving Human

To accurately track humans in a multi-target environment, we must solve two problems. First, we need to quantify the relationship between the scattering pattern produced by a human and that human's location. Second, we need to properly *segment* the returned signal into intervals that isolate the scatter components from individual targets, and *associate* each path component to its generating target. The first problem is modeling issue. We show below that the second problem is implicitly solved by our filtering approach.

Because the relationship between human location/posture and the scattered waveform is complex, we chose an empirical modeling approach rather than a detailed first-principles modeling procedure to investigate the characteristics of moving human scatters.

In order to understand the basic scattering behavior, an experiment was conducted outdoors in an open field containing no clutter in the observation volume. A monostatic UWB radar was collocated on the same vertical axis below a short range LADAR[1] as a ranging reference. The experimental setup

[1]The radar measurements were conducted using a Time Domain PulsOn 210 monostatic radar (TDR) with a waveform sampling period of ~41.33 ps. For the calibration and human measurements, the number of scans acquired was 120 and 3729, respectively. The scanning frequency was 30.7 scans/sec, and the height of the radar was 0.51 m. The LADAR measurements were conducted using a SICK AG short range LIDAR with the operating frequency of 75 scans/sec on every angle from 0° to 180°. The height of the LADAR was 1.32 m. The human object was an adult, 1.77 m tall and 80 kg in weight.

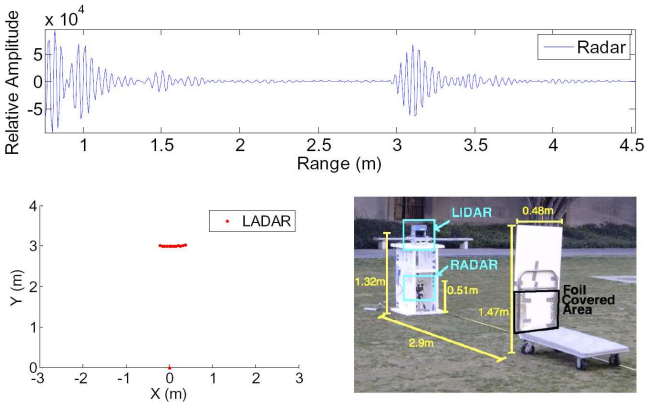

Fig. 2. Scattered UWB waveform, LADAR measurement, and setup picture of the calibration measurement.

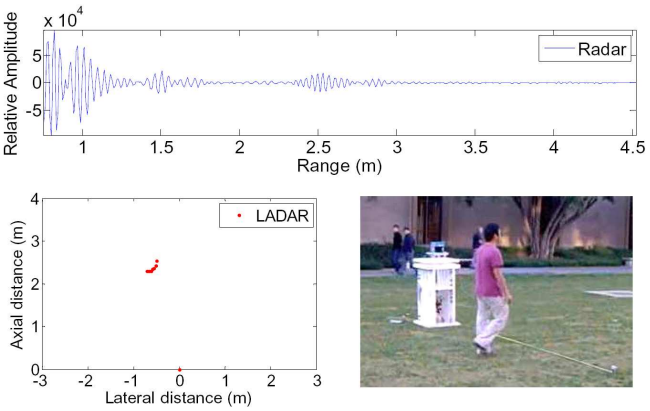

Fig. 3. Scattered UWB waveform, LADAR measurement, and setup picture of the human measurement.

was first calibrated by measuring its response to a styrofoam sheet at 2.90 m far from sensors, where the lower part of the styrofoam sheet was covered by aluminum foil to enable radar reflection in Figure 2. The average waveform of 120 radar scans was processed by the MTI system to cancel direct antenna coupling, and then the MTI response was processed using the CLEAN algorithm with a template waveform in Figure 1 to estimate the TOA of the radar reflection from the sheet. The estimated range of the sheet was 3.10 m by the radar measurement, and 3.00 m by the LADAR measurement (0.10 m offset). Next we constructed a database of UWB radar scans obtained while a human walked randomly in an open field within the vicinity of the radar and the LADAR sensors, where the experimental setup was same as the calibration setup, except without the styrofoam sheet (see Figure 3).

The radar returns were calibrated and processed using the CLEAN algorithm to extract the amplitudes and TOAs of the scattering components. These returns were then manually segmented to ensure a correct data association between detected scatter paths and the human target. The human target's nominal range is defined as the first moment of the power range profile

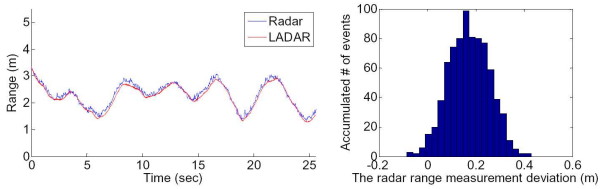

Fig. 4. The radar and LADAR human range measurement comparison.

r [1]:

$$r = \frac{\sum_{j\in\Omega} R_j (a_j R_j^2)^2}{\sum_{j\in\Omega} (a_j R_j^2)^2} \tag{2}$$

where $R_j = [n_j \cdot c]/2$ is the j^{th} scattering path's range[2], and Ω is a set of path indices associated with the human target. Figure 4 shows an empirical distribution histogram of the difference of the nominal radar human range measurement (defined by Equation (2)) and the LADAR human range measurement. The LADAR human range measurement is obtained as follows. the average of multiple LADAR returns corresponding to the cross section of human at the LADAR scanning height was computed and deemed to be the human's location. Compared to the reference LADAR range measurement, the radar human range measurement had a bias with the mean of 0.1722 m and the standard deviation of 0.0841 m. The positive deviation in radar human range measurement may result from the fact that UWB radar signal can penetrate through cloths, and possibly experience wave refraction. Note also that while the LADAR and radar are located along a common vertical axis, their differing heights leads to a small range discrepancy.

Finally, it is convenient to introduce an *adjusted TOA* (ATOA) variable:

$$\delta_j = cn_j/2 - r + K, \tag{3}$$

where n_j is the TOA of the j^{th} scatter component, r is the range to the human, and K is a constant offset related to the delay spread of a typical human. Figure 5 shows the bivariate histogram of the normalized path magnitudes and ATOAs for the human scattering paths in our database. Since the scattered path amplitude is inversely proportional to the square of the scatterer's range, we normalized the path amplitudes to a common 1 meter range reference, i.e., $a(cn/2)^2$, where n is the TOA of that path.

Figure 5 shows that multi-path scatter components are not a particularly strong function of scatter amplitude. Thus, to a good approximation, the mono-static UWB radar scattering process for walking humans, under the specular multipath model in Equation (1), can be interpreted as *point process* governing the ATOAs. After studying common univariate distributions, we found that the ATOA histogram was best fit by a *Gamma distribution* whose mode lies at the human target location and whose probability density function $f_\Gamma(\delta;\kappa,\theta)$ is:

$$f_\Gamma(\delta;\kappa,\theta) = \delta^{\kappa-1}\frac{\exp(-\delta/\theta)}{\theta^\kappa \Gamma(\kappa)} \quad \text{for} \quad \delta > 0, \tag{4}$$

[2]We refer to TOA and range interchangeably in the paper

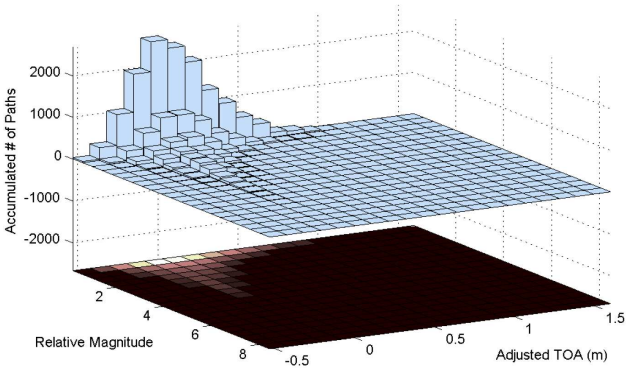

Fig. 5. Empirical distribution of normalized amplitudes and ATOAs of decomposed multipath components for human scatters.

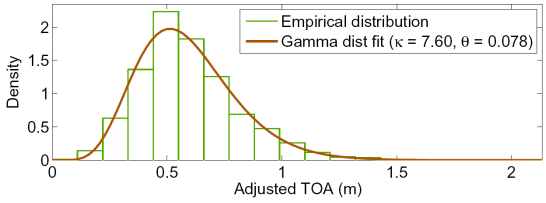

Fig. 6. Histogram of multi-path ATOA, with Gamma distribution fit.

where $\Gamma(\cdot)$ is the Gamma function, and κ, θ are respectively the Gamma distribution's *shape* and *scale* parameters[3]. In our application, the κ parameter is a fixed value characteristic of humans, which is estimated from the database at $\kappa = 7.60$ in Figure 6. The θ parameter is related to target location, and is estimated during the tracking process. While our choice of the Gamma distribution was based on an empirical study, we note that the Gamma distribution exactly models the distribution of arrival times for Poisson distributed events. It is thus a plausible model for human scatter ATOAs.

IV. Tracking a Single Human Target

In light of Section III, human target tracking using mono-static UWB radar can be posed as a classical estimation problem with the twist that the measurements (the TOAs/ATOAs extracted from the return signal) form a point process whose statistics are related to the underlying state variables. Eden et. al [9] have developed a *point process filter* to incorporate point process measurements into a Kalman Filter (KF) framework. The linearization required by their theory is too crude for our application, and thus we take a different approach which uses a Maximum-Likelihood procedure to compute a *derived state measurement* from the point process data.

A. Maximum Likelihood Kalman Filter (MLKF) Algorithm

For simplicity, this section focuses on the case of an ever-present single human target, while the next section considers the multi-target case. Define the state vector $\mathbf{x}$ of a human target as $\mathbf{x} = [r \;\; v]^T$, where r and v respectively denote

[3]All empirical ATOA are adjusted to be positive with $K = 0.533$ m.

the range and velocity (time rate of change of the range) of the human target, and $(\cdot)^T$ denotes the transpose. Then, the tracking problem is to estimate the state vector $\mathbf{x}_k$ in the k^{th} radar scan from the ATOA measurements of the scattered path components associated with the human target in successive scans.

We start with a traditional KF framework, whose dynamic process model is a simple 2^{nd} order random walk:

$$\begin{bmatrix} r_{k+1} \\ v_{k+1} \end{bmatrix} = \begin{bmatrix} 1 & T_s \\ 0 & 1 \end{bmatrix} \begin{bmatrix} r_k \\ v_k \end{bmatrix} + \begin{bmatrix} 0 \\ 1 \end{bmatrix} w_1, \qquad (5)$$

where $T_s = (scan\ frequency)^{-1}$ is the delay between two successive radar scans and $w_1 \sim \mathcal{N}(0, q^2)$ represents Gaussian process noise on the human's velocity. For convenience, Equation (5) can be expressed as:

$$\mathbf{x}_{k+1} = A_k\ \mathbf{x}_k\ +\ \mathcal{W}_1; \quad \text{with} \quad \mathcal{W}_1 \sim \mathcal{N}(\mathbf{0}, Q),$$

where $Q = \mathrm{diag}(0, q^2)$. Because the available measurements are samples of a point process, we cannot construct a typical Kalman Filter measurement equation. Our approach is to construct a *derived measurement* equation as

$$y_k = \begin{bmatrix} 1 & 0 \end{bmatrix} \begin{bmatrix} \hat{r}_k^{ML} \\ v_k \end{bmatrix} + \mathcal{W}_{2,k} = H\mathbf{x}_k + \mathcal{W}_{2,k},$$

where y_k is the "measurement" of human range derived from the k^{th} radar scan, and $\hat{r}_k^{ML}$ is the maximum likelihood range measurement determined by iterative estimation of the θ parameter (see below). The measurement noise $\mathcal{W}_{2,k}$ combines three error sources: conventional measurement noise, error in the CLEAN algorithm, and error due to the ML estimation of $\hat{r}_k^{ML}$. We model the distribution of total measurement error as $\mathcal{W}_{k,2} \sim \mathcal{N}(0, R_k)$ where $R_k = R_{fixed} + R_{ML,k}$ with R_{fixed} denoting the variance due to the first two error sources while $R_{ML,k}$ is the ML estimation error variance, described below.

Letting $\hat{\mathbf{x}}_{k|l}$ and $P_{k|l}$ respectively denote the state estimate and its error covariance at time k given measurements up to time l, the Maximum Likelihood Kalman Filter (MLKF) algorithm for one update follows:

The MLKF Algorithm

1. *Input* : TOAs $\{n_{j,k}\}_{j=1}^N$ of human target's scattering paths.
2. *Initialize* : Set a Gamma distribution parameter κ, offset K, error parameter R_{fixed}, and iteration threshold T_{ML}. Set counter $i = 0$.
3. *Dynamic propagation step* : Given the estimate $\hat{\mathbf{x}}_{k-1|k-1}$ with $P_{k-1|k-1}$ at time $k-1$,calculate the state estimate $\hat{\mathbf{x}}_{k|k-1}$ and its covariance $P_{k|k-1}$ at time k as

$$\begin{aligned} \hat{\mathbf{x}}_{k|k-1} &= A\hat{\mathbf{x}}_{k-1|k-1}, \\ P_{k|k-1} &= AP_{k-1|k-1}A^T + Q. \end{aligned}$$

Set the initial estimate of human range $\hat{r}_k^{(0)} = \hat{r}_{k-1}^{ML}$.
4. *ML estimation* : Compute the ML estimate of the Gamma distribution scale parameter as

$$\hat{\theta}_{ML}^{(i)} = \frac{1}{\kappa N} \sum_{j=1}^{N} \delta_{j,k}^{(i)}$$

where the computed ATOAs are $\delta_{j,k}^{(i)} = cn_{j,k}/2 - \hat{r}_k^{(i)} + K$. The range estimate $\hat{r}_k^{(i+1)}$ in the $(i+1)^{th}$ iteration is at the mode of the Gamma distribution as in Equation (3):

$$\hat{r}_k^{(i+1)} = (\kappa - 1)\hat{\theta}_{ML}^{(i)} + \hat{r}_k^{(i)} - K.$$

5. *Iteration Criterion* : If $|\hat{r}_k^{(i+1)} - \hat{r}_k^{(i)}| > T_{ML}$, go to step 4 with $i \leftarrow i + 1$. Otherwise, set the ML estimate of the range $\hat{r}_k^{ML}$ and the ML estimation error variance $R_{ML,k}$ as

$$\hat{r}_k^{ML} = \hat{r}_k^{(i+1)} \quad \text{and} \quad R_{ML,k} = [(\kappa - 1)\hat{\theta}_{ML}^{(i)}]^2/\kappa N.$$

6. *Measurement Update* : Set the human range measurement $y_k = \hat{r}_k^{ML}$, and compute total measurement noise variance $R_k = R_{fixed} + R_{ML,k}$. Update the Kalman gain K_k, the a posterior state estimate $\hat{\mathbf{x}}_{k|k}$, and the error covariance $P_{k|k}$ as

$$\begin{aligned} K_k &= P_{k|k-1}H^T(HP_{k|k-1}H^T + R_k)^{-1}, \\ \hat{\mathbf{x}}_{k|k} &= \hat{\mathbf{x}}_{k|k-1} + K_k(y_k - H\hat{\mathbf{x}}_{k|k-1}), \\ P_{k|k} &= (I - K_kH)P_{k|k-1}. \end{aligned} \qquad (6)$$

B. Experimental Results

To test the MLKF algorithm, UWB mono-static radar measurement was conducted for a human target who walked straight up to the radar at a nearly uniform velocity, turned around, and then walke away from the radar. The radar scanning period T_s was 0.0786 sec/scan = (12.7 scans/sec)$^{-1}$, and the waveform sampling resolution was 41.33 ps with the range resolution of 0.0062 m. The radar returns were processed using the CLEAN algorithm with T_{clean} = 5×10^4 and the template waveform in Figure 1 to extract the amplitudes and TOAs of the scattering components. These returns were then manually segmented to ensure a correct data association between detected scatter paths and the human target. As a reference, human range was simultaneously measured by a collocated LADAR with the scanning frequency of 75 Hz.

The radar measurement was tested to the MLKF algorithm with parameters of $\kappa = 7.60$, $K = 0.533$ m, $q = 0.0865$ m/s and $R_{fixed} = 0.33$ m^2. Figure 7 shows that the estimated range (the first row of $\hat{\mathbf{x}}_{k|k}$) obtained by using Equation (6) has a strong agreement with the LADAR range measurement, as well as the radar range observation $\hat{r}_k^{ML}$ in Equation (6). The disagreement in the beginning is resulted from the initial velocity assignment in the human state, which was 0 m/s. The velocity estimate (the second row of $\hat{\mathbf{x}}_{k|k}$) by using Equation (6) was effectively close to the linear-fit of the instantaneous target velocity obtained by the LADAR range measurement.

V. Tracking Multiple Human Targets

In the multi-target case, if the human targets are well separated in range, it is easy to segment the return signal into intervals that contain the path components from individual targets. The MLKF algorithm from Section IV could then be applied to the segmented data in order to effect multi-target tracking. However, when the targets overlap in range, we must additionally solve the problem of associating each path component with the 'correct' generating human source. Instead of

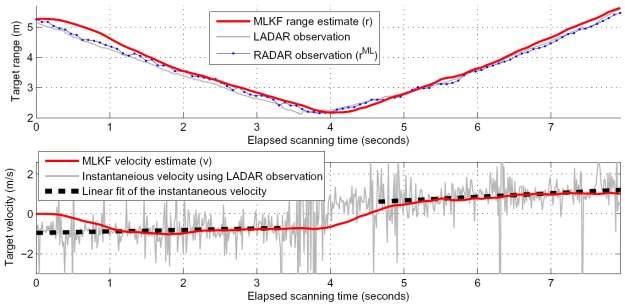

Fig. 7. The MLKF tracking result on a single human target.

using a sequential approach to first solve the data association problem and then solve the measurement estimation problem via the ML method, we choose a probabilistic approach, based on cluster optimization via Expectation Maximization (EM), to jointly solve these problems. The EM algorithm output is then combined with a KF as before.

A. The Combined Kalman Filter and Expectation Maximization (EMKF) Algorithm

Suppose there are G human targets in the observation environment. For a radar scan measurement, Let $Y = \{n_j\}_{j=1}^{M}$ be the set of all scattering path TOA observations with respect to G humans under the specular multipath model in Equation (1). For the TOA observations Y, we define the set of all ATOAs Ω with respect to G humans as

$$\Omega = \bigcup_{g=1}^{G} \{\delta_j^g\}_{j=1}^{M}$$

where the ATOA δ_j^g is a function of the TOA n_j with respect to the g^{th} human range r^g and computed by $\delta_j^g = cn_j/2 - r^g + K$ as in Equation (3)[4]. To generalize the results in Section III, each ATOA subset associated with individual humans' scattering paths may be represented as a component in the mixture model of G Gamma distributions. Hence, including all M TOAs in Y and all mixture components associated with human target index $g = 1, \cdots, G$, the *mixture likelihood* $\mathcal{L}_m$ of the model parameters given the data is:

$$\mathcal{L}_m(\Theta) = p(Y|\Theta) = \prod_{j=1}^{M} \sum_{g=1}^{G} \pi_g f_\Gamma(\delta_j^g; \kappa, \theta_g), \qquad (7)$$

where the form of the model parameters $\Theta = \{\theta_g, \pi_g\}_{g=1}^{G}$, and the mixture weight π_g of the g^{th} component is the prior probability that an observed ATOA was associated with the g^{th} human, with $\pi_g \geq 0$ and $\sum_{g=1}^{G} \pi_g = 1$. If one knew the actual mixture parameters Θ that governed the above model, then each ATOA $\delta \in \Omega$ could be assigned to the g^{th} human whose component likelihood $\pi_g f_\Gamma(\delta; \kappa, \theta_g)$ is the greatest. However, no closed-form solution for the optimal mixture parameters exists using Equation (7) without already knowing which human is associated with each ATOA. Thus, the expectation-maximization (EM) algorithm [10] is typically applied to estimate the parameters, using the following technique [11]. The data Y are considered "incomplete" and are augmented by Z, the set of component-label vectors $\mathbf{z}_j = (z_{j1}, \cdots, z_{jG})$ that indicated TOA membership to a particular human target,

$$z_{jg} = \begin{cases} 1 & \text{if } n_j \text{ is associated with the } g^{th} \text{ human} \\ 0 & \text{otherwise} \end{cases}.$$

Incorporating Z one can derive the corresponding *complete-data log-likelihood*

$$l_{CD}(\Theta|Y, Z) = \sum_{j=1}^{M} \sum_{g=1}^{G} z_{jg} \log[\pi_g f_\Gamma(\delta_j^g; \kappa, \theta_g)], \qquad (8)$$

The EM algorithm iteratively solves for the mixture model parameters Θ and the ATOA membership Z, and will converge to the local optimal estimates of $\hat{\Theta}$ and $\hat{Z}$ [12]. The combined KF and EM algorithm (EMKF) follows closely from the MLKF algorithm, especially for the steps in Kalman Filtering. Letting $\hat{\mathbf{x}}_{k|l}^g$ and $P_{k|l}^g$ respectively denote the state estimate and its error covariance for the g^{th} human target at time k given measurements up to time l, the EMKF algorithm for the time $k-1$ and k follows:

The EMKF Algorithm

1. *Input* : TOAs $Y = \{n_{j,k}\}_{j=1}^{M}$ of G humans scattering paths.
2. *Initialize*: Set a Gamma distribution parameter κ, offset K, measurement noise variance $R = R_{fixed}$, the initial mixture model parameter estimate $\hat{\Theta}^{(0)} = \{\hat{\theta}_g^{(0)}, \pi_g^{(0)}\}_{g=1}^{G}$, and convergence criterion T_{EM}. Set iteration counter $i = 0$.
3. *Dynamic propagation step* : Given the estimate $\hat{\mathbf{x}}_{k-1|k-1}^g$ with $P_{k-1|k-1}^g$ at time $k-1$, calculate the state estimate $\hat{\mathbf{x}}_{k|k-1}^g$ and its covariance $P_{k|k-1}^g$ at time k as

$$\begin{aligned} \hat{\mathbf{x}}_{k|k-1}^g &= A\hat{\mathbf{x}}_{k-1|k-1}^g, \\ P_{k|k-1}^g &= AP_{k-1|k-1}^g A^T + Q. \end{aligned}$$

Set the initial estimate of the human range $\hat{r}_k^{g,(0)} = \hat{r}_{k-1}^{g,EM}$.
4. *EM E-step* : Using the current i^{th} iteration parameter estimates $\hat{\Theta}^{(i)}$ and measurements Y, compute the conditional expectation $\hat{z}_{jg}^{(i+1)} = E[z_{jg}|n_{j,k}, \hat{\Theta}^{(i)}] \in [0, 1]$ as

$$\hat{z}_{jg}^{(i+1)} = \frac{\pi_g f_\Gamma(\delta_{j,k}^{g,(i)}; \kappa, \hat{\theta}_g^{(i)})}{\sum_{n=1}^{G} \pi_g f_\Gamma(\delta_{j,k}^{g,(i)}; \kappa, \hat{\theta}_n^{(i)})},$$

where the ATOAs are calculated by the current i^{th} iteration human range estimate as $\delta_{j,k}^{g,(i)} = cn_{j,k}/2 - \hat{r}_{k|k-1}^{g,(i)} + K$.
5. *EM M-step* : Find the parameter estimates $\hat{\Theta}^{(i)}$ that maximizes the *complete-data log-likelihood* function in Equation (8), given $\hat{z}_{jg}^{(i+1)}$. Using the Lagrange multiplier method with the constraint of $\pi_g \geq 0$ and $\sum_{g=1}^{G} \pi_g = 1$, one obtains

[4]The number of ATOAs is hypothetically expended to be GM by replicating M number of TOAs G times. The EMKF algorithm tests all GM ATOAs to assign only M ATOAs to G humans, effectively.

the following estimates of θ_g and π_g:

$$\hat{\pi}_g^{(i+1)} = \frac{\sum_{j=1}^{M} \hat{z}_{jg}^{(i+1)}}{M} \quad \text{and} \quad \hat{\theta}_g^{(i+1)} = \frac{\sum_{j=1}^{M} \hat{z}_{jg}^{(i+1)} \delta_j^{g,(i)}}{\kappa \sum_{j=1}^{M} \hat{z}_{jg}^{(i+1)}} .$$

The range estimate at the mode of the distribution is:

$$\hat{r}_k^{g,(i+1)} = (\kappa - 1)\hat{\theta}_g^{(i+1)} + \hat{r}_k^{g,(i)} - K.$$

6. *Iteration criterion* : If $\sum_{g=1}^{G} |\hat{r}_k^{g,(i+1)} - \hat{r}_k^{g,(i)}| > T_{EM}$, go to step 4 with $i \leftarrow i+1$. Otherwise, the clustering of TOAs by assigning each TOA $n_{j,k}$ to the g^{*th} human via

$$g^* = \arg\max_g \hat{z}_{jg}.$$

Set the estimate of human range $\hat{r}_k^{g,EM} = \hat{r}_k^{g,(i+1)}$.

7. *Measurement Update* : Set the human range measurement $y_k^g = \hat{r}_k^{g,EM}$. Update the Kalman gain K_k^g, the a posterior state estimate $\hat{\mathbf{x}}_{k|k}^g$, and the error covariance $P_{k|k}^g$ as

$$\begin{aligned} K_k^g &= P_{k|k-1}^g H^T (H P_{k|k-1}^g H^T + R)^{-1}, \\ \hat{\mathbf{x}}_{k|k}^g &= \hat{\mathbf{x}}_{k|k-1}^g + K_k^g (y_k^g - H\hat{\mathbf{x}}_{k|k-1}^g), \\ P_{k|k}^g &= (I - K_k^g H) P_{k|k-1}^g. \end{aligned}$$

B. Experimental Results

To test the EMKF algorithm, UWB mono-static radar measurement was conducted for two human targets. One human walked straight up to the radar at a nearly uniform velocity, and the other human walked straight away from the radar at another nearly uniform velocity at a different angle. The radar scanning period T_s was 0.0786 sec/scan = (12.7 scans/sec)$^{-1}$, and the waveform sampling resolution was 41.33 ps with the range resolution of 0.0062 m. The radar returns were processed using the CLEAN algorithm with T_{clean} = 5×10^4 and the template waveform in Figure 1 to extract the amplitudes and TOAs of the scattering components. As a reference, human range was simultaneously measured by a collocated LADAR with the scanning frequency of 75 Hz.

The radar measurement was tested to the EMKF algorithm with parameters of $\kappa = 7.60$, $K = 0.533$ m, $q = 0.0865$ m/s and $R_{fixed} = 0.1$ m^2. Figure 8 shows that the estimated range has a strong agreement with the LADAR range measurement, even though the targets *overlap* in range at around 1.6 seconds. Also, the velocity estimate was effectively close to the linear-fit of the instantaneous target velocity obtained by the LADAR range measurement.

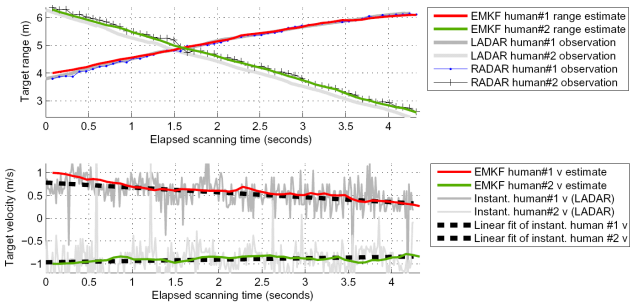

Fig. 8. The EMKF tracking result on two human targets.

VI. Discussion and Conclusion

We introduced the novel observation that monostatic UWB radar multipath scatters from walking humans can be modeled as a point process. Integrating the point process nature of the data into a Kalman Filter framework via an EM mixture model framework allowed for a natural procedure to segment radar returns, associate scatter paths to generating targets, and provided smooth range and velocity estimates for multiple simultaneous human targets. As described in Section V, our algorithm assumes a fixed and known number of human targets. The extension of our approach to a variable number of humans, and to environments that are additionally populated with moving non-human targets can be realized by the application of a recently developed Multi-Hypothesis Cluster Tracking algorithm [11]. While it is beyond the scope of this summary paper, the implementation of this algorithm for UWB radar-based human tracking, is the subject of ongoing work.

References

[1] S. Chang, N. Mitsumoto, J.W. Burdick, "An algorithm for UWB radar-based human detection," (submitted) *Proc. 2009 IEEE Radar Conference (RadarCon09)*, Pasadena, CA, May 2009.

[2] M. I. Skolnik, *Radar Handbook*, New York: McGraw Hill, 1970.

[3] P. Z. Peebles, Jr., *Radar Principles*, New York: Wiley, 1998.

[4] R. M. Narayanan, "Through-Wall Radar Imaging using UWB Noise Waveforms," *J. Franklin Institute* vol. 345, no. 6, pp. 659-678, Sept. 2008.

[5] C. Chang, and A. Sahai, "Object tracking in a 2D UWB sensor network," *Proc. 38th Asilomar Conf. on Signals, Systems and Computers*, vol. 1, pp. 1252-1256, 2004.

[6] R. A. Scholtz, D. M. Pozar, and W. Namgoong, "Ultra-Wideband Radio, *EURASIP Journal of Applied Signal Processing*, No. 3, 2005, pp. 252-272. 5. G. Franceschetti, C.

[7] H. Hashemi, "Impulse response modeling of the indoor radio propagation channels," *IEEE Trans. Select. Areas Commun.*, vol. 11, no. 7, Sep. 1993.

[8] S. M. Yano, "Investigating the ultra-wideband indoor wireless channel," in *Proc. IEEE VTC Spring Conf.*, vol. 3, pp. 1200.1204, 2002.

[9] U.T. Eden, L.M. Frank, V. Solo, and E.N. Brown, "Dynamic Analysis of Neural Encoding by point Process Adaptive Filtering," *Neural Computation* vol. 16, pp. 971-998, 2004.

[10] A. P. Dempster, N. M. Laird, and D. B. Rubin, "Maximum likelihood from incomplete data via the EM algorithm," *Journal of the Royal Statistical Society, Series B*, 39(1):1-38, 1977.

[11] M.T. Wolf, "Target Tracking Using Clustered Measurements, with Applications to Autonomous Brain-Machine Interfaces," *Ph.D. thesis*, Department of Mechanical Engineering, California Institute of Technology, Pasadena, CA, June 2008.

[12] G. McLachlan and D. Peel, *Finite Mixture Models*, Wiley Interscience, 2000.